Title

Ranking of Ligand Binding Kinetics using a Weighted Ensemble Approach and Comparison with Milestoning

Journal

Biophysical Journal, 118(3)

ISSN

0006-3495

Authors

Ahn, Surl-Hee
Jagger, Benjamin
Amaro, Rommie E

Publication Date

2020-02-01

DOI

10.1016/j.bpj.2019.11.1725

Ranking of Ligand Binding Kinetics Using a Weighted Ensemble Approach and Comparison with a Multiscale Milestoning Approach

Surl-Hee Ahn,* Benjamin R. Jagger,* and Rommie E. Amaro*

Department of Chemistry and Biochemistry, University of California San Diego, La Jolla, CA 92093, U.S.A.

E-mail: s3ahn@ucsd.edu; bjagger@ucsd.edu; ramaro@ucsd.edu

Abstract

In order to improve lead optimization efforts in finding the right ligand, pharmaceutical industries need to know the ligand's binding kinetics, such as binding and unbinding rate constants, which often correlate with the ligand's efficacy *in vivo*. To predict binding kinetics efficiently, enhanced sampling methods, such as milestoning and the weighted ensemble (WE) method, have been used in molecular dynamics (MD) simulations of these systems. However, a comparison of these enhanced sampling methods in ranking ligands has not been done. Hence, a WE approach called the concurrent adaptive sampling (CAS) algorithm that uses MD simulations was used to rank seven ligands for β-cyclodextrin, a system in which a multiscale milestoning approach called simulation enabled estimation of kinetic rates (SEEKR) was also used, which uses both MD and Brownian dynamics simulations. Overall, the CAS algorithm can successfully rank ligands using the unbinding rate constants k_{off}'s and binding free energies ΔG's, as SEEKR did, with reduced computational cost that is about the same as SEEKR. We compare the CAS algorithm simulations with different parameters and discuss the

impact of parameters in ranking ligands and obtaining rate constant and binding free energy estimates. We also discuss similarities and differences and advantages and disadvantages of SEEKR and the CAS algorithm for future use.

Introduction

For rational drug optimization, several thermodynamic and kinetic properties may need to be computed *a priori*, such as binding free energies ΔG's, binding rate constants k_{on}'s, and unbinding rate constants k_{off}'s. These properties can indicate the proportion of drug bound to the target and inform on drug binding and unbinding mechanisms, which can help us gain a comprehensive understanding of the drug and its overall effectiveness.[1–4] Although most of these properties can be obtained experimentally, obtaining them for numerous drugs or ligands for each target or receptor can be expensive in terms of time and resources. In addition, detailed understanding of side chain movement and induced fit upon ligand binding or unbinding may not be experimentally tractable. Hence, molecular dynamics (MD) simulations can be helpful to test various ligands with different receptors efficiently.

Nonetheless, MD simulations are not without problems even without the force field issue. Since MD simulations have to be run using femtosecond timesteps, running simulations can be computationally costly if the ligand has a high binding affinity and its residence time (defined to be $1/k_{\text{off}}$) is seconds to minutes or longer. To overcome this "timescale gap," several enhanced sampling and multiscale methods have been applied to various receptor-ligand systems to compute relevant properties quickly,[5–7] including the weighted ensemble (WE) method,[8–16] milestoning,[17–19] metadynamics,[20–24] Markov state models (MSMs),[25–29] steered molecular dynamics (SMD),[30–32] and accelerated molecular dynamics (aMD).[33,34]

Although different enhanced sampling methods have been applied for the same system, e.g., trypsin (receptor) and benzamidine (ligand),[10,18,22,27] there has not yet been a head-to-head study where one enhanced sampling method was applied in ranking or classifying several ligands and compared with another enhanced sampling method in terms of accuracy,

convergence, and efficiency. This can be useful since it is often unclear which enhanced sampling method to use for a given system. In addition, most enhanced sampling methods have parameters that the user has to set *a priori*, which often can be tricky to set optimally. Hence, it is also beneficial to run several of the same simulations with different parameters and report and discuss observations so that we are aware of the impact of parameters.

In this paper, we report ligand ranking results for β-cyclodextrin, a cyclic oligosaccharide compound from starch degradation that is often used as a model receptor, using a WE approach called concurrent adaptive sampling (CAS) algorithm, which uses MD simulations.[35,36] The structure of β-cyclodextrin with its seven glucopyranose units and the seven tested ligands are shown in Figure 1a, Figure 1b, and Figure 1c. β-cyclodextrin is composed of 147 atoms and has a hydrophobic cavity that is 65 $\mathring{A}$ in diameter and a hydrophilic rim with its hydroxyl groups.[37] The reaction process with β-cyclodextrin and its ligand is identified as a second order reaction process described by the following

$$R + L \underset{k_{\text{off}}}{\overset{k_{\text{on}}}{\rightleftharpoons}} RL \tag{1}$$

where R represents the receptor β-cyclodextrin, L represents the ligand, and RL represents the receptor-ligand complex. k_{on} represents the binding rate constant and k_{off} represents the unbinding rate constant. With k_{on} and k_{off}, the binding free energy ΔG can be computed with the following

$$\frac{k_{\text{on}}}{k_{\text{off}}} = Ce^{-\Delta G/RT} \tag{2}$$

where C is a factor equal to 1 with inverse concentration units, R represents the gas constant, and T represents the temperature.

This particular system was previously tested with a multiscale milestoning approach called simulation enabled estimation of kinetic rates (SEEKR), which uses both MD and Brownian dynamics (BD) simulations.[17–19] Ref. 19 reported SEEKR's effectiveness in ranking seven ligands for β-cyclodextrin and "best practices" for SEEKR for its future use. This

paper's reports will parallel those of Ref. 19 so that a direct comparison between the two enhanced sampling methods can be made. Pros and cons of each method will also be discussed in case one method is more appropriate for a particular system over the other. Finally, the CAS algorithm simulations with different parameters will be compared so that the effects of parameters in ranking ligands and obtaining rate constant and binding free energy estimates will be apparent. A recent preprint[38] reported "best practices" for using the WE method to calculate k_{on}, k_{off}, and dissociation constant K_D, including that increasing the target number of walkers per macrostate n_w generally increases the efficiency in obtaining those properties. The preprint, however, mostly focused on different implementations of the WE method, e.g., keeping track of past history and "recycling" trajectories depending on whether reactant/product states are defined or not, and used efficiency as a measure of performance. In addition, Ref. 39 had discussed about the importance of setting the simulation time τ to be longer than the macrostate's relaxation time before reaching steady state, but it did not report results with different τ's. Furthermore, Ref. 40 reported general guidelines for choosing WE method parameters optimally. This paper also discusses about setting the target number of walkers n_w and the simulation time τ optimally, but it also looks into initial structure sampling interval τ_s and simulation time points t where we start analysis of trajectories. This paper uses ranking results and deviations from experimental values as measures of performance.

Methods

Concurrent adaptive sampling algorithm

The CAS algorithm is a WE approach that has several improvements over the original implementation.[41] For details on the original WE method, please refer to Ref. 41, and for details on the CAS algorithm, please refer to Ref. 35. To briefly summarize the WE method, it is an enhanced sampling method that can obtain both thermodynamic properties

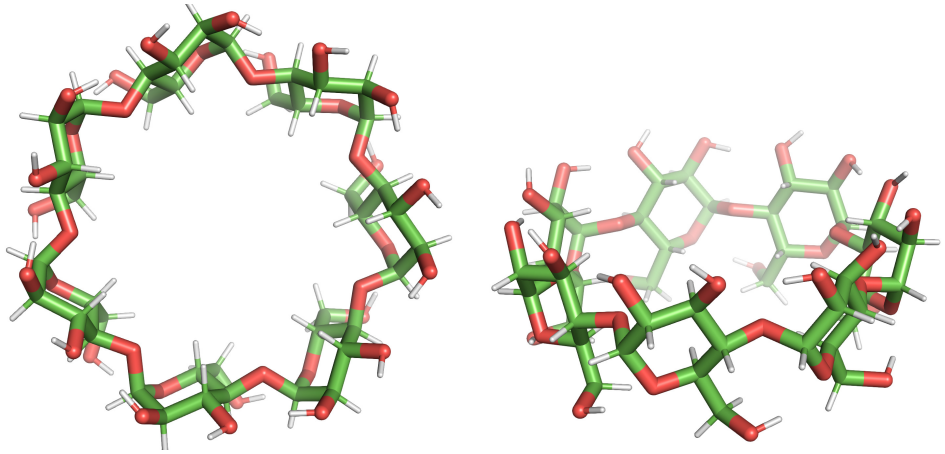

(a) (b)

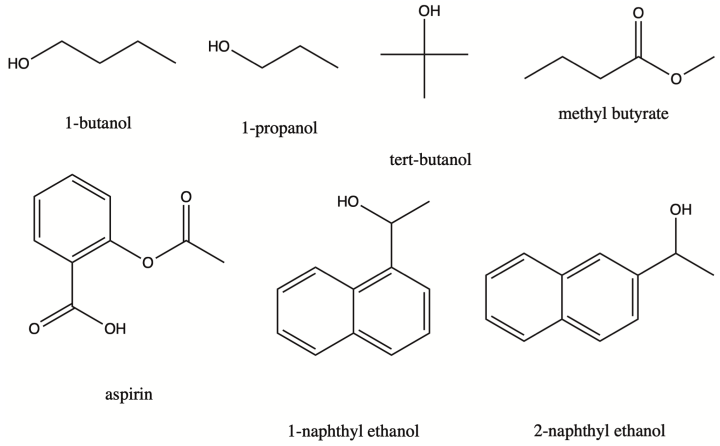

(c)

Figure 1: Structure of β-cyclodextrin and seven tested ligands. (a) shows β-cyclodextrin's secondary face, whereas (b) shows β-cyclodextrin from side. (c) shows the seven tested ligands for this study.

like free energies and kinetic properties like rates and pathways.[42] The WE method works by running many short simulations or "walkers" that carry probabilities or weights and replicating or merging them after every simulation so that the visited parts of the free energy landscape are constantly sampled throughout the simulation. This aspect is crucial since the simulation is able to reach high energy regions with its many walkers and constantly sample those regions with the replicating/merging process (referred to as "resampling") and sample rare events as a result. In addition, the WE method does not add any statistical bias to the system, so we are able to obtain thermodynamic and kinetic properties directly from the simulation without having to use any post-processing methods. Furthermore, the WE method has been successfully applied to protein-ligand systems with pharmacologically relevant timescales[8,10,13]and proteins with folding times in the microsecond to second range and yielded accurate dynamics.[43]

However, the WE method is not without problems so many variants have been developed. First, the original WE method is not able to handle high-dimensional spaces without creating an intractable number of "macrostates" or small volume elements of the conformational space. Hence, adaptive Voronoi cells have been used in several works[35,44,45] so that an intractable number of macrostates do not have to be created beforehand. Multi-dimensional reaction coordinates have also been used in other works[8,35,46,47] so that the computational cost does not dramatically increase. This is useful for systems where we do not know what the true reaction coordinates are. Moreover, there are variants that have extra features that accelerate the sampling process. For instance, the WExplore method divides up the conformational space hierarchically so that rare conformations and events can be sampled efficiently.[9,10,13,46,48] Additionally, the resampling of ensembles by variance optimization (REVO) method creates walkers that maximize variance between them without having defined macrostates, which reduces correlation.[12,47] Finally, the CAS algorithm uses "spectral clustering" that can focus its computational effort in sampling the process going from A to B and vice versa, where A and B are pre-defined metastable states in the

system.[35]

For the particular system that we study in this paper, however, the special features of the CAS algorithm were not needed, so the CAS algorithm essentially reduced down to the regular WE method. The only difference is in the resampling portion, where the walkers end up with equal mean weights, which is proven to be optimal since it reduces statistical errors.[49] In addition, in order to use the CAS algorithm/WE method, a few parameters need to be set *a priori*. However, since the SEEKR runs of β-cyclodextrin with its seven ligands had some of the same parameters set *a priori*, such as the macrostate size (1.5 $\mathring{A}$ in diameter) and reaction coordinate (center of mass distance between the receptor and the ligand), the only parameters that needed to be set were target number of walkers per macrostate n_w and simulation time τ. The target number of walkers per macrostate n_w should be set so that it is large enough to constantly sample the visited macrostates. It is also important to set n_w to be large enough so that the macrostates reach relaxation faster.[39] However, if n_w is set to be too large, then many replications can occur during resampling if walkers in the macrostate are much less than n_w. This causes correlation effects that can slow down convergence.[50] As for simulation time τ, it should not be set to be too long so that transitions are inadvertently missed. However, τ would be ideally longer than the macrostate's relaxation time so that the system reaches relaxation faster and accurate rates are obtained more quickly, especially if the initial states are far from steady state.[39]

Simulation enabled estimation of kinetic rates

SEEKR is a milestoning approach that uses MD simulations in regions where the receptor and the ligand are close together, where atomistic detail is essential to accurately describe the binding and unbinding. Computationally less expensive BD simulations are used in regions where the receptor and ligand are far apart and the binding process is primarily comprised of electrostatically steered diffusion. For details on milestoning, please refer to Ref. 51–56, and for details on SEEKR, please refer to Ref. 17–19. In essence, milestoning is

a path-finding algorithm that mainly focuses on estimating kinetic properties, like pathways and rates, quickly from state A to state B and vice versa. A reaction coordinate is chosen *a priori* that measures the progress going from A to B and vice versa. Milestones are defined as surfaces: $S_1(A), ..., S_{i-1}, S_i, S_{i+1}, ..., S_n(B)$ from state A to state B. If the milestones are defined as isosurfaces of the committor function as in "optimal" or "exact" milestoning, the mean first passage times (MFPT) calculated are exact and milestones can be placed close together for maximum computational efficiency.[56,57] Otherwise, milestones must be spaced sufficiently far apart to ensure that the system decorrelates between successive milestone transitions and MFPTs calculated are approximate. If the milestones are too far apart, however, then the method loses efficiency. For each milestone, a number of trajectories are generated following the Boltzmann distribution. Then the trajectories in each milestone are run independently in parallel until they reach the previous milestone S_{i-1} or the next milestone S_{i+1}. After a sufficient number of trajectories reach adjacent milestones, then the probabilities going from S_i to S_j within a given time t can be computed and overall kinetics can be computed with a transition matrix. The unbinding rate constant k_{off} is calculated as the inverse of the MFPT from the bound state to the outermost MD milestone. From the transition matrix, the stationary probabilities or equilibrium weights of each milestone can also be computed, so thermodynamic properties can also be obtained from milestoning. The binding rate constant k_{on} is calculated using the BD simulations, following the Northrup-Allison-McCammon (NAM) method.[58] The MD transition matrix is combined with the BD transition probabilities and used to determine the steady state flux through the bound state milestone. This probability can be multiplied by the rate of the ligand touching a surface of radius b (which is where the BD simulations are initiated) to determine k_{on}. This approach allows for quick and efficient sampling of a large portion of the association trajectory with BD, an analytical solution for the rate of the ligand approaching from solution, and a more detailed MD description to capture the final steps of binding.

Transition interface sampling (TIS)[59–61] and forward flux sampling (FFS)[62–64] are related

path-sampling algorithms similar to milestoning. The two methods do not need to have surfaces that are sufficiently separated so that the system loses correlation, so the methods have less assumption and can be applied more generally compared to milestoning. Note that FFS can only sample in one direction, however, which is mainly useful for non-equilibrium systems where detailed balance does not hold and backward integration is not possible. The two methods also require sequential processing of trajectories, whereas milestoning can run trajectories in parallel. Since we are interested in computing both k_{on} and k_{off} for receptor-ligand systems, TIS and milestoning would be more preferable for our particular problem. Given that good milestones can be constructed relatively easily, then milestoning would be a suitable method to use. Moreover, the milestoning approach SEEKR can assess convergence of each milestone "on the fly" and extend or terminate trajectories accordingly. Hence, given good milestones and BD simulations for far apart, diffusive regions, SEEKR is a suitable method for computing k_{on}'s and k_{off}'s and ranking ligands, as demonstrated in Ref. 19.

Simulation protocol

β-cyclodextrin along with the seven tested ligands (three tighter binding ligands with slower k_{off}'s on the order of 10^6 (s^{-1}): 1-naphthyl ethanol, 2-naphthyl ethanol, aspiring, and four weaker binding ligands with faster k_{off}'s on the order of $10^7 - 10^9$ (s^{-1}): methyl butyrate, *tert*-butanol, 1-butanol, 1-propanol) were all simulated with NAMD 2.12[65] with time step $\Delta t = 2$ fs. Since the force field q4MD-CD[66] is custom-made for cyclodextrins and agrees better with experimental values[19,37] compared to the generalized Amber force field (GAFF),[67] q4MD-CD was used for β-cyclodextrin and GAFF was used for the seven ligands. TIP3P explicit solvent[68] was used to solvate all of the seven different receptor-ligand systems. The LEaP program from Amber 16[69] was used to generate parameters and topologies for the seven receptor-ligand systems. Most simulation parameters were identical to the ones in Ref. 19, which is the SEEKR study on the same system, and Ref. 37, which is the brute force MD simulation study on the same system.

To initialize each receptor-ligand system, the SEEKR software package was used. As done in SEEKR, the following steps were done for initialization.

1. Each system was set to have ten spherical macrostates with a diameter of 1.5 $\mathring{A}$ or a radius of 0.75 $\mathring{A}$, where the distance represented the center of mass distance between the receptor and the ligand, which is the same as the milestones in SEEKR. The ten macrostates ranged from $0.0 - 1.5$ $\mathring{A}$, $1.5 - 3.0$ $\mathring{A}$, ..., $12.0 - 13.5$ $\mathring{A}$, and $13.5 - 15.0$ $\mathring{A}$. Since the current CAS algorithm software package does not have BD simulations integrated with it, unlike SEEKR, the last macrostate $13.5 - 15.0$ $\mathring{A}$ in reality held all of the walkers where the receptor and the ligand were 13.5 $\mathring{A}$ or more separated.

2. Each receptor-ligand conformation was minimized for 5000 steps to allow for relaxation. Only the solvent was allowed to be minimized since the receptor-ligand distances needed to be kept.

3. Then each receptor-ligand conformation went through a series of 2 ps heating simulations that gradually increased the temperature from 298 K to 350 K and then cooled back to 298 K. Again, the receptor and the ligand were constrained during the simulations.

4. To minimize the time to extract initial structures for the CAS algorithm simulation, only 50 ns of NVT equilibrium simulation at 298 K with Langevin thermostat (damping coefficient 5.0 ps^{-1}) was run for each receptor-ligand conformation, instead of 200 ns as done in SEEKR. Note that SEEKR had carried out NVE simulations whereas the CAS algorithm carried out NVT simulations since stochastic dynamics are essential for walkers to carry out dynamics without any bias. The dynamics in the NVT ensemble should not be drastically different from those in the NVE ensemble, however. The distance between the receptor and the ligand was constrained with 90 $kcal/(mol \cdot \mathring{A}^2)$ harmonic force so that various structures with similar receptor-ligand distances could be obtained for each macrostate. Since there were ten macrostates in total, the total

equilibrium simulation time ended up to be 500 ns. The first 40 ns were disregarded as equilibration time for each conformation, so only the last 10 ns were used to extract initial structures for each macrostate.

5. Finally, the CAS algorithm simulation was run under the NVT ensemble at 298 K with Langevin thermostat (damping coefficient 5.0 ps^{-1}) for 3200 ns so that the total simulation time, along with the equilibrium simulation time, will be ~ 3.7 μs, as done in SEEKR. Three independent CAS algorithm runs were run for each simulation so that the reported error bars reflect the true uncertainty.

In the CAS algorithm simulation, the ten macrostates were fixed throughout the simulation. For each CAS algorithm simulation, the initial structures were extracted either at every 100 or 200 ps from the last 10 ns of equilibrium simulation for each macrostate. The initial structure sampling interval will be denoted as τ_s from hereinafter. All of the initial structures carried equal weights. If the initial structures were from the first five macrostates with $0.0 - 1.5$ $\mathring{A}$, ..., $6.0 - 7.5$ $\mathring{A}$, then those structures were colored as "blue." Conversely, if the initial structures were from the last five macrostates with $7.5 - 9.0$ $\mathring{A}$, ..., $13.5 - 15.0$ $\mathring{A}$, then those structures were colored as "red." The walkers would keep the colors that they started out with until they reached a different state from their current state, i.e., "blue" would turn "red" (unbound state) if the receptor-ligand distance was 13.5 $\mathring{A}$ or higher and "red" would turn "blue" (bound state) if the receptor-ligand distance was 1.5 $\mathring{A}$ or lower. The definitions for the bound and unbound states are the same as those used in SEEKR so that we could directly compare results. Note that the initial assignment of colors could bias rates, but it was done because it appeared to speed up convergence of rates in preliminary studies (data not shown). Resampling was also done separately for each color so that there would be the same number of walkers for each color in each macrostate. This coloring scheme was used to calculate the flux going from bound to unbound and vice versa directly from the CAS algorithm simulation, as done in several WE method works.[35,36,42,70–72] The total simulation time was calculated by the cumulative number of macrostates $\times$ target number of walkers

per macrostate n_w × simulation time τ. The target number of walkers per macrostate n_w was set to either 100 or 200. The simulation time τ was set to either 100 or 200 ps. The parameters for each CAS algorithm simulation runs are listed in Table 1.

Table 1: Parameters for each CAS algorithm simulation runs

Condition Set #	τ_s	n_w	τ
1	100 ps	100	100 ps
2	100 ps	100	200 ps
3	100 ps	200	100 ps
4	200 ps	100	100 ps

Data analysis

The binding rate constants k_{on}'s and unbinding rate constants k_{off}'s, were calculated using

$$k_{\text{on}} = \frac{1}{[\text{solute}] \times \text{average unbound time}} \tag{3}$$

$$k_{\text{off}} = \frac{1}{\text{average bound time}} \tag{4}$$

where [solute] represents the solute concentration, which is calculated for each receptor-ligand system. This is the same as done in Ref. 37, which calculated the same β-cyclodextrin rate constants with the seven tested ligands using brute force MD simulation. The average bound and unbound times were calculated using the Hill relation,[73] i.e., the average transition times are equal to the inverses of the fluxes, respectively. We can use this relation because we used colors to keep track of the walkers' transitions and resampled each color separately. Alternatively, we could have re-inserted the walkers that go from the bound state to the unbound state and vice versa to reach steady state.[39,74] The fluxes were calculated using

$$\text{flux}_{\text{bound to unbound}} = \frac{1}{n}\sum_{i=1}^{n}\frac{1}{\tau}\frac{\sum \text{weights of all blue walkers that turn red at step } i}{\sum \text{weights of all blue walkers at step } i} \tag{5}$$

$$\text{flux}_{\text{unbound to bound}} = \frac{1}{n}\sum_{i=1}^{n}\frac{1}{\tau}\frac{\sum \text{weights of all red walkers that turn blue at step } i}{\sum \text{weights of all red walkers at step } i} \tag{6}$$

where n denotes the total number of simulation steps and τ denotes the simulation time. However, for more accurate calculations of binding rate constants k_{on}'s, the NAM method should be implemented in the CAS algorithm in the future, as done in SEEKR and in other WE works.[41,75–77] The values for [solute] for each receptor-ligand system and details on how it was calculated is in the SI. Note that the BD simulations in SEEKR were only used to simulate the region where the receptor and the ligand were far apart from each other, which is a reasonable approximation, and only came into play in calculating the k_{on}'s. The region where the receptor and the ligand were close to each other was simulated with MD simulations in both the CAS algorithm and SEEKR. Hence, the k_{off}'s from the CAS algorithm and SEEKR can be directly compared with each other. The binding free energies ΔG's were calculated using the calculated k_{on}'s, k_{off}'s, and Eq. 2 with $T = 298\ K$.

The error bars for k_{on}'s, k_{off}'s, and ΔG's are standard errors obtained from the three independent CAS algorithm runs. The Kendall tau and Spearman rho correlation coefficients were used to measure how well the CAS algorithm ranked the ligands in terms of k_{on}'s, k_{off}'s, and ΔG's compared to experiments. Both correlation coefficients range from -1 to 1 where 1 represents identical correlation (i.e., two rankings are the same), whereas -1 represents fully different correlation (i.e., two rankings are completely the opposite). Kendall tau is based on the numbers of concordant (same ranking) and discordant (opposite ranking) pairs, whereas Spearman rho is based on deviations in rankings. The two correlation coefficients and associated error bars were calculated using an in-house Python script that was used in Ref. 19, which calculated the same β-cyclodextrin rate constants with the seven tested ligands using SEEKR.

The k_{on}'s and ΔG's were also alternatively calculated using probabilities. According to Ref. 45, the ratio of transition probabilities gives the ratio of equilibrium populations of two regions, i.e.,

$$\frac{N_{\text{bound}}}{N_{\text{unbound}}} = \frac{p_{\text{unbound}\to\text{bound}}}{p_{\text{bound}\to\text{unbound}}} \tag{7}$$

where N denotes the equilibrium population and p denotes the transition probability. The

transition probabilities are given from the flux matrices that are written out at every simulation step in the CAS algorithm simulation. Hence, with Eq. 7, the ratio $k_{\text{on}}/k_{\text{off}}$ can be rewritten as

$$\frac{k_{\text{on}}}{k_{\text{off}}} = \frac{p_{\text{unbound}\rightarrow\text{bound}}}{p_{\text{bound}\rightarrow\text{unbound}} \times [\text{solute}]} \tag{8}$$

Hence, by using Eq. 8, which is another expression for Eq. 2, we can compute ΔG and if we plug in the given k_{off} values, which are more accurate and will be discussed in the next sections, then alternative values for k_{on} can be obtained.

Finally, the initial structures can bias the estimates of rate constants and free energies.[71] Hence, three simulation time points ($t = 0, 400, 800$ ns) where we start analysis of trajectories were tested to see how it affects the estimates of rate constants and free energies.

Results

The CAS algorithm gave comparable ranking results to SEEKR and brute force MD simulations.

Similar to brute force MD simulations and SEEKR, the CAS algorithm failed to rank ligands accurately with k_{on}'s as seen in Figure 2a, which shows the best k_{on} results from the CAS algorithm simulations in terms of ranking and rate constant estimates. The other CAS algorithm simulation results are reported in the SI. The k_{on}'s are all one order of magnitude larger than the experimental values, and the rankings have low or negative Kendall tau and Spearman rho correlation coefficients as seen in Table 2. As stated in Ref. 19, the k_{on} values are all within half an order of magnitude, which makes ranking difficult for both experiments and computational methods. Note that even though the k_{on}'s were calculated differently in the CAS algorithm and in SEEKR, the results are similar in terms of ranking and value estimates.

However, the CAS algorithm successfully ranked ligands with k_{off}'s and ΔG's, which differ

1 kcal or less for most cases, as seen in Figure 3a and Figure 4a, which show the best k_{off} and ΔG results from the CAS algorithm simulations, respectively, in terms of ranking and rate constant estimates. The other CAS algorithm simulation results are reported in the SI. The k_{off}'s and ΔG's both also had high Kendall tau and Spearman rho correlation coefficients as seen in Table 3 and Table 4. Like SEEKR, the CAS algorithm was also able to differentiate between the three tighter binding ligands (aspirin, 1-naphthyl ethanol, 2-naphthyl ethanol) from the four weaker binding ligands (methyl butyrate, *tert*-butanol, 1-butanol, 1-propanol), which have at least one order of magnitude difference from each other in terms of k_{off}. In addition, since k_{off} values for the seven ligands span over multiple orders of magnitude, it is easier to rank ligands using k_{off}, as stated in Ref. 19.

Moreover, the k_{off} ranking converged after 1000 ns, as seen in Figure 3b. Hence, to get accurate ligand ranking results using k_{off}'s, then as little as < 2 μs of total simulation time per ligand is needed using the CAS algorithm, which is similar to SEEKR. The k_{off} ranking for other runs converged at different times, ranging from 1000 ns to less than 2500 ns for the seven runs that had the highest Kendall tau and Spearman rho correlation coefficients of 0.9 and 0.96, respectively which are reported in the SI. Similarly, the ΔG ranking converged for all of the runs except for one (Condition Set #3 with $t = 0$ ns), which are reported in the SI. On the other hand, the k_{on} ranking did not converge for any of the runs, except for two (Condition Set #2 with $t = 0$ ns and Condition Set #3 with $t = 0$ ns), which are reported in the SI. When comparing the Kendall tau and Spearman rho correlation coefficients, calculating the k_{on}'s and ΔG's with probabilities did not give better results as seen in Figure 2b and Figure 4b. Hence, this alternative method for calculating k_{on}'s and ΔG's can be used but it is not guaranteed to yield better results.

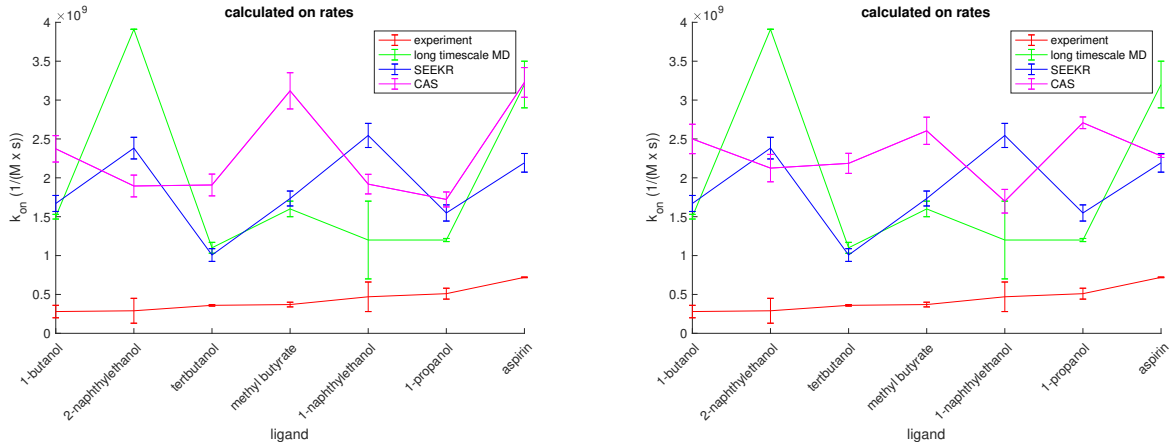

(a) (b)

Figure 2: k_{on} ranking results. (a) shows results from Condition Set #4 with $t = 400$ ns, and (b) shows results from Condition Set #1 with $t = 800$ ns using probabilities. The error bars are standard errors obtained from the three independent CAS algorithm runs.

Table 2: k_{on} ranking results

Simulation method	Kendall tau	Spearman rho
Brute force MD	0 ± 0.28	-0.05 ± 0.37
SEEKR	0.14 ± 0.29	0.14 ± 0.38
CAS (#4 with $t = 400$ ns)	0.14 ± 0.22	0.18 ± 0.27
CAS (#1 with $t = 800$ ns using probabilities)	0.14 ± 0.29	0.18 ± 0.38

Table 3: k_{off} ranking results

Simulation method	Kendall tau	Spearman rho
Brute force MD	1 ± 0.05	1 ± 0.03
SEEKR	0.81 ± 0.09	0.93 ± 0.05
CAS (#4 with $t = 400$ ns)	0.9 ± 0.06	0.96 ± 0.04

Table 4: ΔG ranking results

Simulation method	Kendall tau	Spearman rho
Brute force MD	0.87 ± 0.11	0.94 ± 0.06
SEEKR	0.73 ± 0.1	0.89 ± 0.06
CAS (#1 with $t = 400$ ns)	0.81 ± 0.08	0.93 ± 0.05
CAS (#4 with $t = 400$ ns using probabilities)	0.81 ± 0.09	0.93 ± 0.06

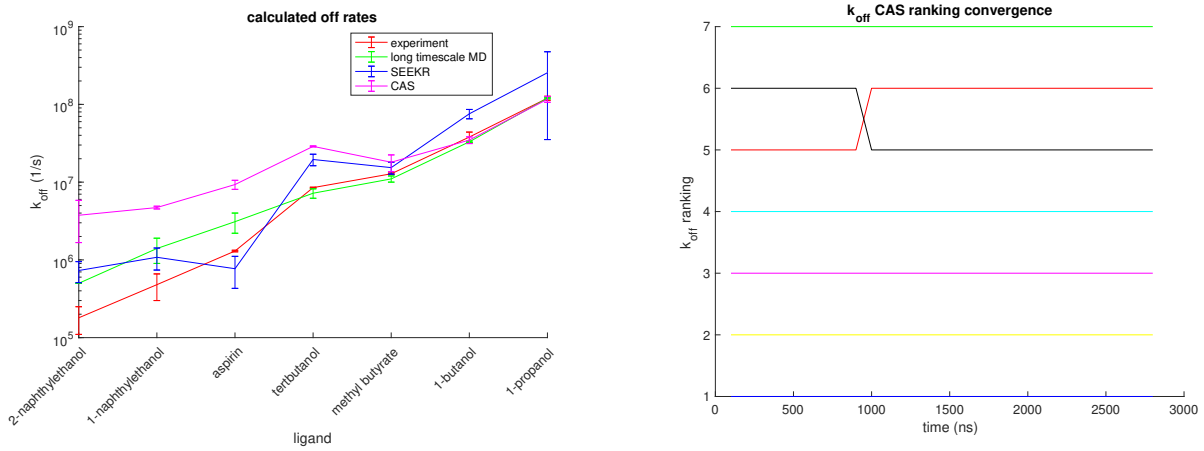

(a) (b)

Figure 3: k_{off} ranking results. (a) shows results from Condition Set #4 with $t = 400$ ns. The error bars are standard errors obtained from the three independent CAS algorithm runs. (b) shows ranking convergence results from Condition Set #4 with $t = 400$ ns. The different colored lines indicate different ligands (red: 1-butanol, yellow: 1-naphthyl ethanol, green: 1-propanol, blue: 2-naphthyl ethanol, magenta: aspirin, cyan: methyl butyrate, black: *tert*-butanol) and the ligand with the lowest k_{off} value gets the highest ranking of 1.

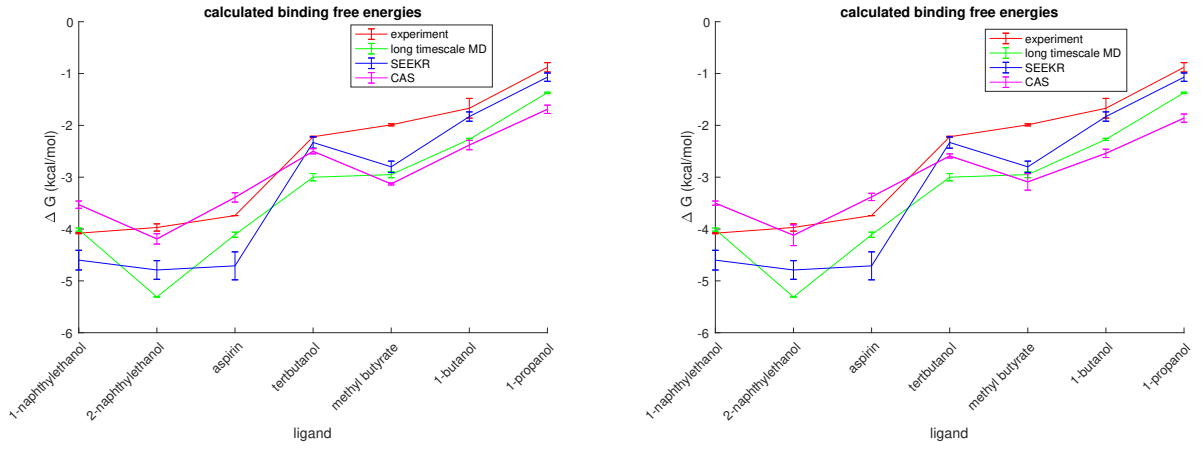

(a) (b)

Figure 4: ΔG ranking results. (a) shows results from Condition Set #1 with $t = 400$ ns, and (b) shows results from Condition Set #4 with $t = 400$ ns using probabilities. The error bars are standard errors obtained from the three independent CAS algorithm runs.

The CAS algorithm yielded more accurate results for $k_{\mathbf{on}}$ and $k_{\mathbf{off}}$ after getting rid of initial structure bias.

Since the initial structures can bias the results, as previously noted in other WE works,[8,42,45,46,71] the rate constants and free energies were calculated at three different simulation time points ($t = 0, 400, 800$ ns) where we start analysis of trajectories for each simulation, as mentioned previously in the Data Analysis section. First, the simulation time points were picked for each simulation that had the highest Kendall tau and Spearman rho correlation coefficients for k_{on}, k_{off}, and ΔG. The results are summarized in Table 5. From Table 5, it is clear that getting rid of initial structure bias is necessary to get the k_{on} ranking as accurately as possible, even though none of the simulations was successful at ranking ligands using k_{on}. Calculating k_{off} and ΔG after some simulation time had passed also improved ranking results for the most part.

Since most simulations had multiple simulation time points that gave the highest Kendall tau and Spearman rho correlation coefficients of 0.9 and 0.96, respectively, for k_{off}, the k_{off} estimates were compared with experimental values to rank which simulation time point was the best in terms of rate constant estimates. Figure 5a summarizes the root-mean-square deviations (RMSDs) from experimental values for the simulations with the simulation time points that had the highest Kendall tau and Spearman rho correlation coefficients of 0.9 and 0.96, respectively, for k_{off}. The RMSD was obtained from the difference between the averaged values from three independent CAS algorithm simulations and the experimental values, so no error bars were reported. Condition Set #3 had lower Kendall tau and Spearman rho correlation coefficients of 0.81 and 0.89, respectively, so it was not included in Figure 5a. For all simulations, having a simulation time point of $t = 400$ ns decreased the RMSD the most as seen in Figure 5a. This indicated that getting rid of initial structure bias improved k_{off} estimates but it can be detrimental if we remove too much.

Similarly, the RMSDs from experimental ΔG values were calculated for the simulations with the starting points that had the highest Kendall tau and Spearman rho correlation

coefficients of 0.81 and 0.93, respectively, and are shown in Figure 5b. Again, the RMSD was obtained from the difference between the averaged values from three independent CAS algorithm simulations and the experimental values, so no error bars were reported. Condition Set #3 had lower Kendall tau and Spearman rho correlation coefficients of 0.71 and 0.86, respectively, so it was not included in Figure 5b. Similar to k_{off}, getting rid of a moderate amount of initial structure bias (t = 400 ns) decreased the RMSD for ΔG (Condition Set #1). However, most simulations needed to have a higher simulation time point of t = 800 ns to rank ligands accurately in the first place using ΔG. This might be because ΔG's are calculated from the ratio of k_{on}'s and k_{off}'s, as stated in Eq. 2, and k_{on}'s might need more initial structure bias to be removed for accurate ranking and estimates.

Taken together, getting rid of initial structure bias improved ranking results and yielded estimates closer to experimental values for k_{off} and ΔG. This is further supported from each ligand's rate constant convergence results, as seen in Figure 6c and Figure 6d, where the simulation time point t = 0 ns is shown to be the slowest at converging to experimental k_{on} and k_{off} values. The rest of the ligand convergence results are reported in the SI. Although it is a standard protocol to start analysis for the later portions of the WE method simulations, as mentioned in previous WE works,[8,42,45,46,71] these results further confirmed the importance of the practice, specifically in terms of ranking ligands and obtaining accurate estimates.

Table 5: Simulation time points that had the highest correlation coefficients

Condition Set #	t for k_{on} (ns)	t for k_{off} (ns)	t for ΔG (ns)
1	400, 800	0, 400, 800	400, 800
2	400, 800	400, 800	800
3	800	0, 400, 800	0, 400, 800
4	0, 400	400, 800	800

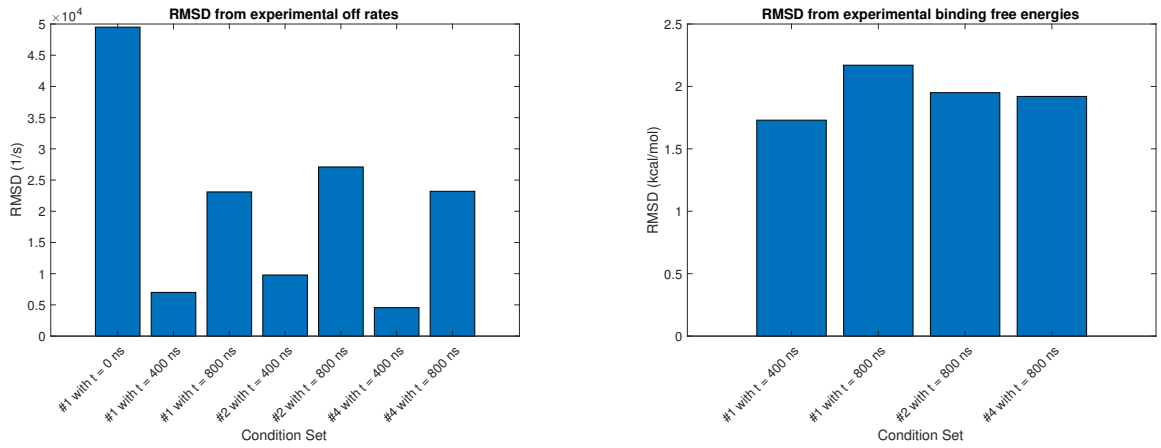

(a) (b)

Figure 5: Root-mean-square-deviations (RMSDs) results. (a) shows the RMSD results from experimental k_{off} values, and (b) shows the RMSD results from experimental ΔG values. The RMSD was obtained from the difference between the averaged values from three independent CAS algorithm simulations and the experimental values, so no error bars were reported.

The CAS algorithm yielded more accurate results after having less correlated initial structures.

As stated previously, Condition Set #3 was the only simulation that did not have the highest Kendall tau and Spearman rho correlation coefficients of 0.96 and 0.96, respectively, for k_{off}, out of the four types of simulations. Similarly, Condition Set #3 was also the only simulation that did not have the highest Kendall tau and Spearman rho correlation coefficients of 0.81 and 0.89, respectively, for ΔG. Condition Set #3 was the only simulation with the larger target number of walkers $n_w = 200$ compared to $n_w = 100$ for the rest of the simulations. Since the initial structure sampling interval τ_s was 100 ps for Condition Set #3, which resulted in 100 initial structures for each macrostate (using 10 ns of brute force simulation data), having $n_w = 200$ resulted in duplicating most of the initial structures. This produced correlated samples, which resulted in less accurate ranking results.

This is further supported from each ligand's rate constant convergence results, as seen in Figure 6a and Figure 6b, where Condition Set #3 is shown to be the slowest at converging to experimental k_{on} and k_{off} values. Similarly, Figure 6e and Figure 6f show that doubling

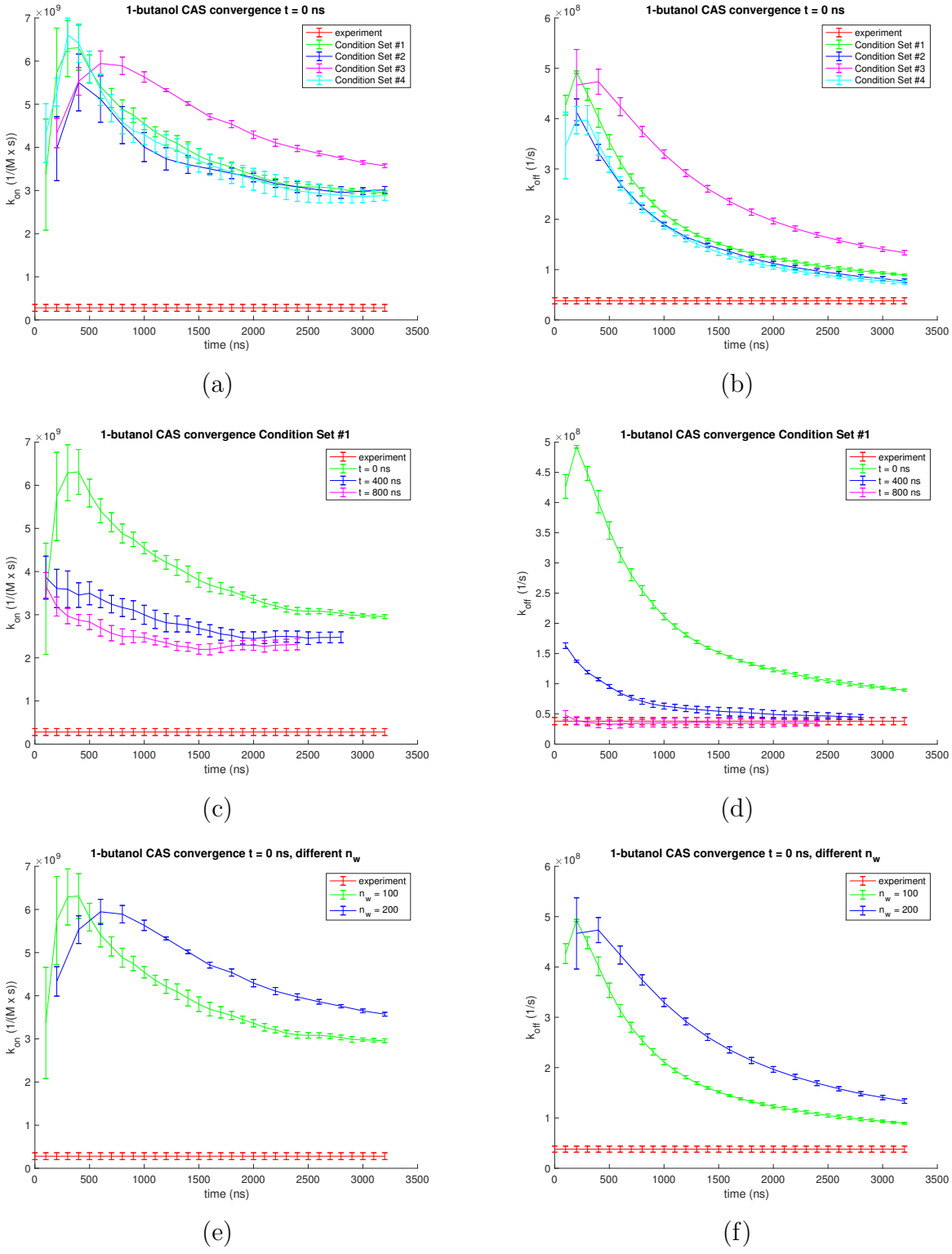

Figure 6: 1-butanol convergence results. (a) shows k_{on} results with $t = 0$ ns for all Condition Sets, and (b) shows k_{off} results with $t = 0$ ns for all Condition Sets. (c) shows k_{on} results for Condition Set #1, and (d) shows k_{off} results for Condition Set #1. (e) shows k_{on} results with $t = 0$ ns and different n_w, and (f) shows k_{off} results with $t = 0$ ns and different n_w.

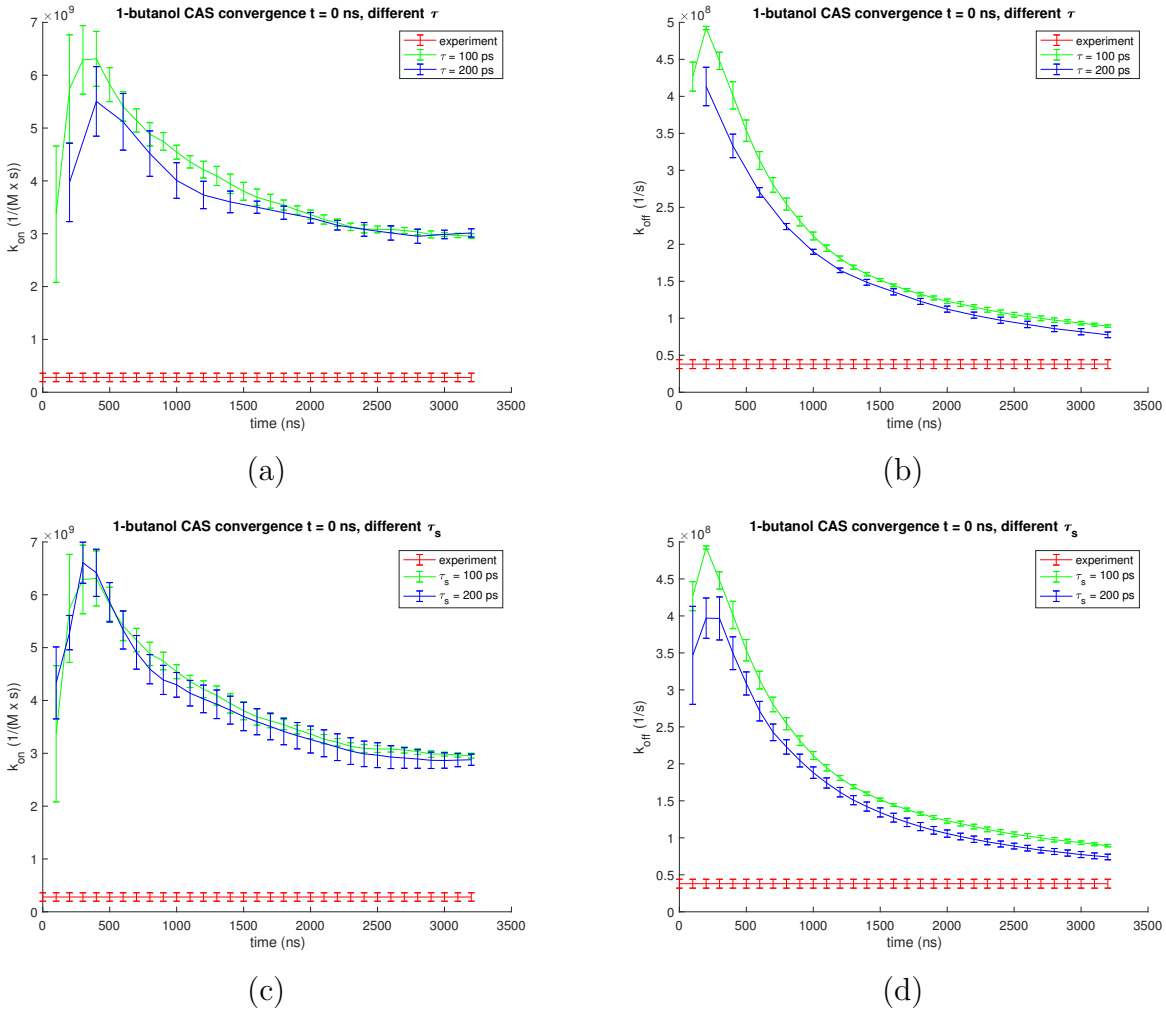

Figure 7: 1-butanol convergence results. (a) shows k_{on} results with $t = 0$ ns and different τ, and (b) shows k_{off} results with $t = 0$ ns and different τ. (c) shows k_{on} results with $t = 0$ ns and different τ_s, and (d) shows k_{off} results with $t = 0$ ns and different τ_s.

n_w from 100 to 200 causes slower convergence for both k_{on} and k_{off}, since we start with 100 initial structures for each macrostate in the first place. These results are consistent with those of Ref. 50. The rest of the ligand convergence results are reported in the SI.

Moreover, Condition Set #4, which was the only simulation that had $\tau_s = 200$ ps, instead of $\tau_s = 100$ ps for the rest of the simulations, yielded the lowest RMSD results for both k_{off} and ΔG compared to the rest of the simulations at the same simulation time point ($t = 0, 400, 800$ ns) for analysis of trajectories, as seen in Figure 5a and Figure 5b. Since Condition Set #4 had a longer τ_s, the initial structures were less correlated, which enabled Condition Set #4 to obtain more accurate rate constant and free energy estimates compared to the rest of the simulations. However, note that the benefit of having a longer τ_s is not apparent in the ligand convergence results, as seen in Figure 7c and Figure 7c, which show similar rate of convergence for both $\tau_s = 100$ ps (Condition Set #1) and $\tau_s = 200$ ps (Condition Set #4). Taken together, having less correlated initial structures is crucial for accurate ranking and rate constant and free energy estimates.

The CAS algorithm should sample transitions more frequently by having shorter simulation times.

Although Ref. 39 noted that the simulation time τ should be longer than the macrostate's relaxation time before reaching steady state, we found that Condition Set #2, which was the only simulation that had a longer simulation time $\tau = 200$ ps compared to the rest of the simulations that had $\tau = 100$ ps, did not yield better results in terms of ranking and rate constant and free energy estimates. Hence, 100 ps was probably sufficiently longer than the macrostate's relaxation time and 200 ps was probably too long so that some transitions were inadvertently missed. Additionally, Condition Set #2 was the only simulation that needed to get rid of initial structure bias for all three calculated properties (k_{on}, k_{off}, and ΔG). This might have been due to less frequent resampling, which could have helped to correct initial structure bias for Condition Set #2. However, τ did not have an effect on convergence, as

seen in Figure 7a and Figure 7b. This is not entirely surprising, however, since τ just needs to be longer than the macrostate's relaxation time to obtain accurate rate constant and free energy estimates.[39] Otherwise, τ serves as a "checking point" for the simulation.

Discussion

The CAS algorithm showed comparable results to those of SEEKR. This is not entirely surprising since both enhanced sampling methods share many similarities. Both methods work by running many short simulations in parallel, which significantly lowers the computational cost compared to brute force MD simulations. Both methods can also simultaneously sample binding rate constants k_{on}'s and unbinding rate constants k_{off}'s and yield results that fall within an order of magnitude of actual values. The results also have small error bars by sampling along the milestones/macrostates at a high rate, which can be controlled by extending the simulation until the desired accuracy and/or convergence is reached. Moreover, both methods require little *a priori* knowledge about the receptor-ligand system since binding and unbinding are determined from the chosen reaction coordinate, which in this case was the distance between the receptor and the ligand (a good, natural choice for studying receptor-ligand systems). But because of this requirement, the choice of reaction coordinate is critical for both methods, which can be difficult for more complex systems. In addition, in order to obtain accurate rate constants, both methods need the initial structures to be from near-equilibrium distributions. This is especially true for SEEKR, which spent most of its simulation time generating initial structures before running the actual milestoning step. The CAS algorithm, on the other hand, spent most of its time running the actual WE method step.

Although SEEKR used both MD and BD simulations whereas the CAS algorithm only used MD simulations, both methods yielded results in reasonable agreement with each other. In SEEKR, BD simulations were only used to calculate k_{on}, and MD transition statistics were

only used to calculate k_{off}, with the assumption that once the ligand is sufficiently far from the receptor (last MD milestone), then the ligand is considered to be unbound. Hence, k_{off}'s are directly comparable as they came from MD simulations in both methods, aside from the fact that the CAS algorithm simulations were in the NVT ensemble and SEEKR simulations were in the NVE ensemble, which should not be drastically different from each other. As for k_{on}'s, the CAS algorithm used the inverse of the average unbound time, which was calculated using the Hill relation. In contrast, SEEKR used the NAM method, which allowed for an analytical treatment of the association process from bulk, combined with the BD binding probability for the outer milestone and the MD binding probability for the inner milestones. The inner milestones were still treated with MD, however, so the free energy landscape for this region is comparable between the two methods. The BD simulations were only used for the outer milestones, with the assumption that the atomistic forces of MD were not needed (no short range interactions and distances are larger than the MD cutoff distance), to reduce sampling costs in a region where MD may not be necessary. Hence, the free energy landscape for the outer milestones is different between the two methods. Depending on which interactions are critical for a particular system (e.g., electrostatic complementarity of the ligand and the receptor, conformational changes needed for binding), BD may produce higher or lower k_{on}'s compared to MD. Nonetheless, the calculated k_{on}'s were in reasonable agreement with each other as seen in the Results section, with both methods and brute force MD simulations overestimating k_{on}'s by one order of magnitude compared to experimental values. Moreover, since both methods failed to rank ligands accurately using k_{on}'s, most of the Results section focused on k_{off}'s and ΔG's, which were mostly determined by k_{off} values since the magnitudes were larger than k_{on} values. As a result, the difference in how the k_{on}'s were calculated did not significantly impact the comparison of the two methods.

When choosing which method to use to obtain binding rate constants k_{on}'s and unbinding rate constants k_{off}'s for receptor-ligand systems, the choice will not matter too much in terms of accuracy and performance. However, if we are somewhat familiar with the receptor-ligand

system, SEEKR will be more suitable because the computational cost is lower than that of the CAS algorithm. With SEEKR, convergence of each milestone can be monitored and simulations can be run or terminated accordingly "on the fly." The CAS algorithm, on the other hand, needs to run all simulations for each macrostate since it requires global convergence of macrostates. However, in order to obtain accurate results from SEEKR, the milestones need to be sufficiently separated so that the system loses memory when it reaches the next milestone, which either requires a bit of knowledge about the receptor-ligand system or confirming the decorrelation of trajectories after an initial short amount of simulation on each milestone.

On the other hand, we do not need to worry about losing accuracy due to how the macrostates are constructed for the CAS algorithm. This is because the Markov assumption is not used[44] and transition pathways are directly computed by each walker keeping track of its past history. Performance (i.e., convergence and efficiency), however, will heavily be affected by how the macrostates are constructed. For instance, if the macrostates are too big, then the walkers will struggle to transition to another macrostate. If the macrostates are too small, then the computational cost will be higher than necessary. Fortunately, performance can be easily improved by letting the CAS algorithm construct macrostates adaptively and/or changing the size of the macrostates in the middle of the simulation. This was not done in this paper, since reasonable macrostates were known *a priori* through previous work using SEEKR,[19] but this could have easily been done if the CAS algorithm had difficulty in sampling transitions. In contrast, because SEEKR terminates trajectories upon crossing a milestone, changing the spacing of the milestones, or a subset of milestones, would require new simulations to be run to sample these transitions.

Conclusions

To find the optimal drug or ligand for a particular target or receptor, pharmaceutical industries need to rank a number of ligands with its kinetic (binding rate constants k_{on}'s and unbinding rate constants k_{off}'s) and thermodynamic (binding free energies ΔG's) properties. In order to obtain these properties in a timely and cost efficient manner, the various receptor-ligand systems should be simulated with enhanced sampling methods. SEEKR, a multiscale milestoning approach that uses both MD and BD simulations, is one enhanced sampling method that demonstrated its effectiveness in tackling this issue. We showed that another method, the CAS algorithm, a WE method approach that uses MD simulations, is another effective enhanced sampling method that shows comparable results to those of SEEKR. Both enhanced sampling methods needed $3.7 - 3.8$ μs per ligand (or as little as < 2 μs for some ligands) to obtain accurate rankings compared to $4.5 - 11$ μs per ligand using regular MD simulations.[37] As with any other enhanced sampling method that has parameters that need to be set *a priori*, the CAS algorithm showed variability in terms of accuracy and performance depending on the parameters. Hence, we compared simulations with different parameters and discussed the impact of parameters in ranking ligands and obtaining rate constant and binding free energy estimates using the CAS algorithm. In general, getting rid of initial structure bias and correlated initial structures ensured more accurate results. Additionally, having shorter simulation times so that transitions are sampled more frequently ensured more accurate results. Finally, we discussed similarities and differences of SEEKR and the CAS algorithm and when to use each method for the receptor-ligand system of interest.

Notes

The authors declare the following competing financial interest(s): R.E.A. is a co-founder of, on the scientific advisory board of, and has equity interest in Actavalon, Inc.

Acknowledgement

S.-H.A. acknowledges support from NIH GM31749 and University of California San Diego. B.R.J. acknowledges support from the NIH Molecular Biophysics Training Program (T32-GM008326). This work was funded in part by the National Biomedical Computation Resource (NBCR) NIH P41-GM103426 and the National Science Foundation through XSEDE supercomputing resources provided via TG-CHE060073 to R.E.A. The authors thank J. Andrew McCammon and Gary Huber for helpful discussions and the reviewers for their thorough and detailed reviews that improved the paper.

Supporting Information Available

The CAS algorithm code is available at `http://github.com/shirleyahn/CAS_Code`. The SEEKR code is available at `http://amarolab.ucsd.edu/seekr`. Simulation files are available upon request.

References

(1) Copeland, R. A.; Pompliano, D. L.; Meek, T. D. Drug–target residence time and its implications for lead optimization. *Nat. Rev. Drug Discov.* **2006**, *5*, 730.

(2) Copeland, R. A. The drug–target residence time model: a 10-year retrospective. *Nat. Rev. Drug Discov.* **2016**, *15*, 87.

(3) Tummino, P. J.; Copeland, R. A. Residence time of receptor- ligand complexes and its effect on biological function. *Biochemistry* **2008**, *47*, 5481–5492.

(4) Swinney, D. C. Biochemical mechanisms of drug action: what does it take for success? *Nat. Rev. Drug Discov.* **2004**, *3*, 801.

(5) Bruce, N. J.; Ganotra, G. K.; Kokh, D. B.; Sadiq, S. K.; Wade, R. C. New approaches for computing ligand–receptor binding kinetics. *Curr. Opin. Struc. Biol.* **2018**, *49*, 1–10.

(6) Bernetti, M.; Masetti, M.; Rocchia, W.; Cavalli, A. Kinetics of drug binding and residence time. *Annu. Rev. Phys. Chem.* **2019**, *70*, 143–171.

(7) Amaro, R. E.; Mulholland, A. J. Multiscale methods in drug design bridge chemical and biological complexity in the search for cures. *Nat. Rev. Chem.* **2018**, *2*, 0148.

(8) Zwier, M. C.; Pratt, A. J.; Adelman, J. L.; Kaus, J. W.; Zuckerman, D. M.; Chong, L. T. Efficient atomistic simulation of pathways and calculation of rate constants for a protein–peptide binding process: application to the MDM2 protein and an intrinsically disordered p53 peptide. *J. Phys. Chem. Lett.* **2016**, *7*, 3440–3445.

(9) Dickson, A.; Lotz, S. D. Ligand release pathways obtained with WExplore: residence times and mechanisms. *J. Phys. Chem. B* **2016**, *120*, 5377–5385.

(10) Dickson, A.; Lotz, S. D. Multiple ligand unbinding pathways and ligand-induced destabilization revealed by WExplore. *Biophys. J.* **2017**, *112*, 620–629.

(11) Dickson, A. Mapping the ligand binding landscape. *Biophys. J.* **2018**, *115*, 1707–1719.

(12) Dixon, T.; Lotz, S. D.; Dickson, A. Predicting ligand binding affinity using on-and off-rates for the SAMPL6 SAMPLing challenge. *J. Comput. Aided Mol. Des.* **2018**, *32*, 1001–1012.

(13) Lotz, S. D.; Dickson, A. Unbiased molecular dynamics of 11 min timescale drug unbinding reveals transition state stabilizing interactions. *J. Am. Chem. Soc.* **2018**, *140*, 618–628.

(14) Teo, I.; Mayne, C. G.; Schulten, K.; Lelièvre, T. Adaptive multilevel splitting method

for molecular dynamics calculation of benzamidine-trypsin dissociation time. *J. Chem. Theory Comput.* **2016**, *12*, 2983–2989.

(15) Nunes-Alves, A.; Zuckerman, D. M.; Arantes, G. M. Escape of a small molecule from inside T4 lysozyme by multiple pathways. *Biophys. J.* **2018**, *114*, 1058–1066.

(16) Saglam, A. S.; Chong, L. T. Protein–protein binding pathways and calculations of rate constants using fully-continuous, explicit-solvent simulations. *Chem. Sci.* **2019**, *10*, 2360–2372.

(17) Votapka, L. W.; Amaro, R. E. Multiscale estimation of binding kinetics using Brownian dynamics, molecular dynamics and milestoning. *PLoS Comput. Biol.* **2015**, *11*, e1004381.

(18) Votapka, L. W.; Jagger, B. R.; Heyneman, A. L.; Amaro, R. E. SEEKR: simulation enabled estimation of kinetic rates, a computational tool to estimate molecular kinetics and its application to trypsin–benzamidine binding. *J. Phys. Chem. B* **2017**, *121*, 3597–3606.

(19) Jagger, B. R.; Lee, C. T.; Amaro, R. E. Quantitative ranking of ligand binding kinetics with a multiscale milestoning simulation approach. *J. Phys. Chem. Lett.* **2018**, *9*, 4941–4948.

(20) Limongelli, V.; Marinelli, L.; Cosconati, S.; La Motta, C.; Sartini, S.; Mugnaini, L.; Da Settimo, F.; Novellino, E.; Parrinello, M. Sampling protein motion and solvent effect during ligand binding. *Proc. Natl. Acad. Sci.* **2012**, *109*, 1467–1472.

(21) Söderhjelm, P.; Tribello, G. A.; Parrinello, M. Locating binding poses in protein-ligand systems using reconnaissance metadynamics. *Proc. Natl. Acad. Sci.* **2012**, *109*, 5170–5175.

(22) Tiwary, P.; Limongelli, V.; Salvalaglio, M.; Parrinello, M. Kinetics of protein–ligand unbinding: Predicting pathways, rates, and rate-limiting steps. *Proc. Natl. Acad. Sci.* **2015**, *112*, E386–E391.

(23) Brotzakis, Z. F.; Limongelli, V.; Parrinello, M. Accelerating the calculation of protein–ligand binding free energy and residence times using dynamically optimized collective variables. *J. Chem. Theory Comput.* **2018**, *15*, 743–750.

(24) Haldar, S.; Comitani, F.; Saladino, G.; Woods, C.; van der Kamp, M. W.; Mulholland, A. J.; Gervasio, F. L. A multiscale simulation approach to modeling drug–protein binding kinetics. *J. Chem. Theory Comput.* **2018**, *14*, 6093–6101.

(25) Held, M.; Metzner, P.; Prinz, J.-H.; Noé, F. Mechanisms of protein-ligand association and its modulation by protein mutations. *Biophys. J.* **2011**, *100*, 701–710.

(26) Gu, S.; Silva, D.-A.; Meng, L.; Yue, A.; Huang, X. Quantitatively characterizing the ligand binding mechanisms of choline binding protein using Markov state model analysis. *PLoS Comput. Biol.* **2014**, *10*, e1003767.

(27) Plattner, N.; Noé, F. Protein conformational plasticity and complex ligand-binding kinetics explored by atomistic simulations and Markov models. *Nat. Commun.* **2015**, *6*, 7653.

(28) Thayer, K. M.; Lakhani, B.; Beveridge, D. L. Molecular dynamics–markov state model of protein ligand binding and allostery in CRIB-PDZ: Conformational selection and induced fit. *J. Phys. Chem. B* **2017**, *121*, 5509–5514.

(29) Bernetti, M.; Masetti, M.; Recanatini, M.; Amaro, R. E.; Cavalli, A. An Integrated Markov State Model and Path Metadynamics Approach To Characterize Drug Binding Processes. *J. Chem. Theory Comput.* **2019**, *15*, 5689–5702.

(30) Whalen, K. L.; Chang, K. M.; Spies, M. A. Hybrid Steered Molecular Dynamics-Docking: An Efficient Solution to the Problem of Ranking Inhibitor Affinities Against a Flexible Drug Target. *Mol. Inform.* **2011**, *30*, 459–471.

(31) Patel, J. S.; Berteotti, A.; Ronsisvalle, S.; Rocchia, W.; Cavalli, A. Steered molecular dynamics simulations for studying protein–ligand interaction in cyclin-dependent kinase 5. *J. Chem. Inf. Model.* **2014**, *54*, 470–480.

(32) Vuong, Q. V.; Nguyen, T. T.; Li, M. S. A new method for navigating optimal direction for pulling ligand from binding pocket: application to ranking binding affinity by steered molecular dynamics. *J. Chem. Inf. Model.* **2015**, *55*, 2731–2738.

(33) Hamelberg, D.; Mongan, J.; McCammon, J. A. Accelerated molecular dynamics: a promising and efficient simulation method for biomolecules. *J. Chem. Phys.* **2004**, *120*, 11919–11929.

(34) Miao, Y.; Feher, V. A.; McCammon, J. A. Gaussian accelerated molecular dynamics: Unconstrained enhanced sampling and free energy calculation. *J. Chem. Theory Comput.* **2015**, *11*, 3584–3595.

(35) Ahn, S.-H.; Grate, J. W.; Darve, E. F. Efficiently sampling conformations and pathways using the concurrent adaptive sampling (CAS) algorithm. *J. Chem. Phys.* **2017**, *147*, 074115.

(36) Ahn, S.-H.; Grate, J. W.; Darve, E. F. Investigating the role of non-covalent interactions in conformation and assembly of triazine-based sequence-defined polymers. *J. Chem. Phys.* **2018**, *149*, 072330.

(37) Tang, Z.; Chang, C.-E. A. Binding thermodynamics and kinetics calculations using chemical host and guest: a comprehensive picture of molecular recognition. *J. Chem. Theory Comput.* **2017**, *14*, 303–318.

(38) Pratt, A.; Suárez, E.; Zuckerman, D.; Chong, L. Extensive evaluation of weighted ensemble strategies for calculating rate constants and binding affinities of molecular association/dissociation processes. *bioRxiv* **2019**, 671172.

(39) Bhatt, D.; Zhang, B. W.; Zuckerman, D. M. Steady-state simulations using weighted ensemble path sampling. *J. Chem. Phys.* **2010**, *133*, 014110.

(40) others,, et al. A suite of tutorials for the WESTPA rare-events sampling software. *Living J. Comput. Mol. Sci.* **2019**, *1*, 10607.

(41) Huber, G. A.; Kim, S. Weighted-ensemble Brownian dynamics simulations for protein association reactions. *Biophys. J.* **1996**, *70*, 97–110.

(42) Suárez, E.; Lettieri, S.; Zwier, M. C.; Stringer, C. A.; Subramanian, S. R.; Chong, L. T.; Zuckerman, D. M. Simultaneous computation of dynamical and equilibrium information using a weighted ensemble of trajectories. *J. Chem. Theory Comput.* **2014**, *10*, 2658–2667.

(43) Adhikari, U.; Mostofian, B.; Copperman, J.; Subramanian, S. R.; Petersen, A. A.; Zuckerman, D. M. Computational estimation of microsecond to second atomistic folding times. *J. Am. Chem. Soc.* **2019**, *141*, 6519–6526.

(44) Zhang, B. W.; Jasnow, D.; Zuckerman, D. M. The weighted ensemble path sampling method is statistically exact for a broad class of stochastic processes and binning procedures. *J. Chem. Phys.* **2010**, *132*, 054107.

(45) Bhatt, D.; Bahar, I. An adaptive weighted ensemble procedure for efficient Comput. of free energies and first passage rates. *J. Chem. Phys.* **2012**, *137*, 104101.

(46) Dickson, A.; Brooks III, C. L. WExplore: hierarchical exploration of high-dimensional spaces using the weighted ensemble algorithm. *J. Phys. Chem. B* **2014**, *118*, 3532–3542.

(47) Donyapour, N.; Roussey, N. M.; Dickson, A. REVO: Resampling of ensembles by variation optimization. *J. Chem. Phys.* **2019**, *150*, 244112.

(48) Dickson, A.; Mustoe, A. M.; Salmon, L.; Brooks III, C. L. Efficient in silico exploration of RNA interhelical conformations using Euler angles and WExplore. *Nucleic Acids Res.* **2014**, *42*, 12126–12137.

(49) Schlick, T. *Innovations in Biomolecular Modeling and Simulations*; Royal Society of Chemistry, 2012; Vol. 1.

(50) Zuckerman, D. M.; Chong, L. T. Weighted ensemble simulation: review of methodology, applications, and software. *Annu. Rev. Biophys.* **2017**, *46*, 43–57.

(51) Faradjian, A. K.; Elber, R. Computing time scales from reaction coordinates by milestoning. *J. Chem. Phys.* **2004**, *120*, 10880–10889.

(52) Vanden-Eijnden, E.; Venturoli, M.; Ciccotti, G.; Elber, R. On the assumptions underlying milestoning. *J. Chem. Phys.* **2008**, *129*, 174102.

(53) Májek, P.; Elber, R. Milestoning without a reaction coordinate. *J. Chem. Theory Comput.* **2010**, *6*, 1805–1817.

(54) Vanden-Eijnden, E.; Venturoli, M. Markovian milestoning with Voronoi tessellations. *J. Chem. Phys.* **2009**, *130*, 194101.

(55) Elber, R.; Bello-Rivas, J.; Ma, P.; Cardenas, A.; Fathizadeh, A. Calculating iso-committor surfaces as optimal reaction coordinates with milestoning. *Entropy* **2017**, *19*, 219.

(56) Bello-Rivas, J. M.; Elber, R. Exact milestoning. *J. Chem. Phys.* **2015**, *142*, 03B602_1.

(57) Lin, L.; Lu, J.; Vanden-Eijnden, E. A mathematical theory of optimal milestoning (with a detour via exact milestoning). *Commun. Pur. Appl. Math.* **2018**, *71*, 1149–1177.

(58) Northrup, S. H.; Allison, S. A.; McCammon, J. A. Brownian dynamics simulation of diffusion-influenced bimolecular reactions. *J. Chem. Phys.* **1984**, *80*, 1517–1524.

(59) Bolhuis, P. G. Transition-path sampling of β-hairpin folding. *Proc. Natl. Acad. Sci.* **2003**, *100*, 12129–12134.

(60) Moroni, D.; van Erp, T. S.; Bolhuis, P. G. Investigating rare events by transition interface sampling. *Physica A: Statistical Mechanics and its Applications* **2004**, *340*, 395–401.

(61) Van Erp, T. S.; Bolhuis, P. G. Elaborating transition interface sampling methods. *J. Comput. Phys.* **2005**, *205*, 157–181.

(62) Allen, R. J.; Frenkel, D.; ten Wolde, P. R. Forward flux sampling-type schemes for simulating rare events: Efficiency analysis. *J. Chem. Phys.* **2006**, *124*, 194111.

(63) Valeriani, C.; Allen, R. J.; Morelli, M. J.; Frenkel, D.; Rein ten Wolde, P. Computing stationary distributions in equilibrium and nonequilibrium systems with forward flux sampling. *J. Chem. Phys.* **2007**, *127*, 114109.

(64) Allen, R. J.; Valeriani, C.; ten Wolde, P. R. Forward flux sampling for rare event simulations. *J. Phys.: Condensed Matter* **2009**, *21*, 463102.

(65) Phillips, J. C.; Braun, R.; Wang, W.; Gumbart, J.; Tajkhorshid, E.; Villa, E.; Chipot, C.; Skeel, R. D.; Kale, L.; Schulten, K. Scalable molecular dynamics with NAMD. *J. Comput. Chem.* **2005**, *26*, 1781–1802.

(66) Cézard, C.; Trivelli, X.; Aubry, F.; Djedaïni-Pilard, F.; Dupradeau, F.-Y. Molecular dynamics studies of native and substituted cyclodextrins in different media: 1. Charge derivation and force field performances. *Phys. Chem. Chem. Phys.* **2011**, *13*, 15103–15121.

(67) Wang, J.; Wolf, R. M.; Caldwell, J. W.; Kollman, P. A.; Case, D. A. Development and testing of a general amber force field. *J. Comput. Chem.* **2004**, *25*, 1157–1174.

(68) Jorgensen, W. L.; Chandrasekhar, J.; Madura, J. D.; Impey, R. W.; Klein, M. L. Comparison of simple potential functions for simulating liquid water. *J. Chem. Phys.* **1983**, *79*, 926–935.

(69) Case, D. et al. AMBER16. 2016.

(70) Costaouec, R.; Feng, H.; Izaguirre, J.; Darve, E. Analysis of the accelerated weighted ensemble methodology. *Discrete Cont. Dyn. Syst.* **2013**, 171–181.

(71) Feng, H.; Costaouec, R.; Darve, E.; Izaguirre, J. A. A comparison of weighted ensemble and Markov state model methodologies. *J. Chem. Phys.* **2015**, *142*, 06B610_1.

(72) Suárez, E.; Adelman, J. L.; Zuckerman, D. M. Accurate estimation of protein folding and unfolding times: beyond Markov state models. *J. Chem. Theory Comput.* **2016**, *12*, 3473–3481.

(73) Hill, T. L. *Free energy transduction and biochemical cycle kinetics*; Courier Corporation, 2005.

(74) Donovan, R. M.; Sedgewick, A. J.; Faeder, J. R.; Zuckerman, D. M. Efficient stochastic simulation of chemical kinetics networks using a weighted ensemble of trajectories. *J. Chem. Phys.* **2013**, *139*, 09B642_1.

(75) Rojnuckarin, A.; Livesay, D. R.; Subramaniam, S. Bimolecular reaction simulation using weighted ensemble Brownian dynamics and the University of Houston Brownian dynamics program. *Biophys. J.* **2000**, *79*, 686–693.

(76) Saglam, A. S.; Chong, L. T. Highly efficient computation of the basal k on using direct simulation of protein–protein association with flexible molecular models. *J. Phys. Chem. B* **2015**, *120*, 117–122.

(77) Saglam, A. S.; Wang, D. W.; Zwier, M. C.; Chong, L. T. Flexibility vs preorganization: Direct comparison of binding kinetics for a disordered peptide and its exact preorganized analogues. *J. Phys. Chem. B* **2017**, *121*, 10046–10054.

Graphical TOC Entry